Spironolactone Decreases DOCA–Salt–Induced Organ Damage by Blocking the Activation of T Helper 17 and the Downregulation of Regulatory T Lymphocytes

Cristián A. Amador, Víctor Barrientos, Juan Peña, Andrés A. Herrada, Magdalena González, Solange Valdés, Loreto Carrasco, Rodrigo Alzamora, Fernando Figueroa, Alexis M. Kalergis and Luis Michea

Hypertension. published online January 13, 2014;
Hypertension is published by the American Heart Association, 7272 Greenville Avenue, Dallas, TX 75231

Print ISSN: 0194-911X. Online ISSN: 1524-4563

Spironolactone Decreases DOCA–Salt–Induced Organ Damage by Blocking the Activation of T Helper 17 and the Downregulation of Regulatory T Lymphocytes

Cristián A. Amador,* Víctor Barrientos,* Juan Peña, Andrés A. Herrada, Magdalena González, Solange Valdés, Loreto Carrasco, Rodrigo Alzamora, Fernando Figueroa, Alexis M. Kalergis, Luis Michea

Abstract—Adaptive immune response has been implicated in inflammation and fibrosis as a result of exposure to mineralocorticoids and a high-salt diet. We hypothesized that in mineralocorticoid-salt–induced hypertension, activation of the mineralocorticoid receptor alters the T-helper 17 lymphocyte (Th17)/regulatory T-lymphocyte/interleukin-17 (IL-17) pathway, contributing to cardiac and renal damage. We studied the inflammatory response and tissue damage in rats treated with deoxycorticosterone acetate and high-salt diet (DOCA–salt), with or without mineralocorticoid receptor inhibition by spironolactone. To determine whether Th17 differentiation in DOCA–salt rats is caused by hypertension per se, DOCA–salt rats received antihypertensive therapy. In addition, to evaluate the pathogenic role of IL-17 in hypertension and tissue damage, we studied the effect of IL-17 blockade with a specific antibody (anti–IL-17). We found activation of Th17 cells and downregulation of forkhead box P3 mRNA in peripheral tissues, heart, and kidneys of DOCA–salt–treated rats. Spironolactone treatment prevented Th17 cell activation and increased numbers of forkhead box P3–positive cells relative to DOCA–salt rats. Antihypertensive therapy did not ameliorate Th17 activation in rats. Treatment of DOCA–salt rats with anti–IL-17 significantly reduced arterial hypertension as well as expression of profibrotic and proinflammatory mediators and collagen deposits in the heart and kidney. We conclude that mineralocorticoid receptor activation alters the Th17/regulatory T-lymphocyte/IL-17 pathway in mineralocorticoid-dependent hypertension as part of an inflammatory mechanism contributing to fibrosis. **(*Hypertension*. 2014;63:00-00.)** ● **Online Data Supplement**

Key Words: aldosterone ■ fibrosis ■ hypertension ■ inflammation ■ interleukin-17 ■ receptors, mineralocorticoid

Mineralocorticoid receptor (MR) activation and high salt intake causes hypertension as well as inflammation, leading to cardiovascular and renal fibrosis and remodeling.[1,2] Early studies showed that lymphocytes are necessary for the development of chronic hypertension, perivascular mononuclear cell infiltration, and renal injury in response to deoxycorticosterone acetate and high-salt diet (DOCA–salt).[3] Consequently, transfer of splenic cells from DOCA–salt donor rats to normal rats results in hypertension, mononuclear cell infiltration, and vascular remodeling in heart and kidney.[4] Recently, Guzik et al[5] demonstrated that mice lacking T cells and B cells (Rag-1$^{-/-}$ mice) exhibited blunted hypertension and do not develop vascular dysfunction/remodeling during DOCA–salt or angiotensin II (Ang II) treatment. Adoptive transfer of T cells, but not B cells, to Rag-1$^{-/-}$ mice restored hypertension, endothelial dysfunction, and vascular wall remodeling.[5] Although these results suggest a fundamental role of T cells in hypertension, inflammation, and fibrosis, they do not provide information on the mechanisms underlying T-cell activation or the specific T-cell subsets implicated in MR-dependent hypertension and organ damage.

Interleukin-17 (IL-17) is a proinflammatory cytokine produced mainly by T helper 17 lymphocytes (Th17). Polarization of Th17 depends on differentiation triggers, such as transforming growth factor-β1 (TGF-β1), IL-6, IL-1β, IL-23, and IL-21, acting on naive Th cells.[6,7] IL-17 is found to be upregulated in atherosclerosis[8,9] and myocardial infarction,[10] and the absence/blockade of IL-17 in rodents protects from cardiac remodeling and fibrosis.[11–13] Moreover, Ang II infusion in mice is associated with an increase of Th17, and IL-17$^{-/-}$ mice exhibit a lower hypertensive response to Ang II infusion as compared with wild-type mice.[14] All these data suggest that

Received November 25, 2013; first decision December 10, 2013; revision accepted December 18, 2013.

From the Center for Molecular Studies of the Cell (C.A.A., V.B., J.P., M.G., S.V., L.C., R.A., L.M.) and Millennium Institute on Immunology and Immunotherapy, Departamento de Fisiología y Biofísica, ICBM, Facultad de Medicina (C.A.A., V.B., J.P., M.G., S.V., R.A., L.M.), Universidad de Chile, Santiago, Chile; Departamento de Genética Molecular y Microbiología, Facultad de Ciencias Biológicas, Millennium Institute on Immunology and Immunotherapy and Departamento de Reumatología, Facultad de Medicina, Pontificia Universidad Católica de Chile, Santiago, Chile (A.A.H., A.M.K.); and Facultad de Medicina, Universidad de los Andes, Santiago, Chile (F.F.).

*C.A.A and V.B. are joint first authors.

The online-only Data Supplement is available with this article at http://hyper.ahajournals.org/lookup/suppl/doi:10.1161/HYPERTENSIONAHA.113.02883/-/DC1.

Correspondence to Luis F. Michea, Facultad de Medicina, Universidad de Chile, Independencia 1027, Santiago, Chile. E-mail lmichea@med.uchile.cl

IL-17 may participate in hypertension and fibrosis/remodeling produced by MR activation and a high-salt diet.

Regulatory T lymphocytes (Tregs) modulate the innate and adaptive immune responses.[15] Tregs suppress Th17 polarization and the expression of IL-17 both in vitro and in vivo.[15–17] An imbalance in Th17/Treg function could be implicated in hypertension, inflammation, and organ damage caused by mineralocorticoids and high-salt diet. Recent studies have demonstrated that the hypertension and vascular damage induced by Ang II in mice results in decreased numbers of Treg cells,[18,19] and the adoptive transfer of isolated $CD4^+CD25^+$ lymphocytes enriched in Tregs ameliorated hypertension and suppressed vascular injury attributable to aldosterone+high-salt diet.[20]

To test the hypothesis that an altered activity of Th17/Treg caused by MR activation participates in hypertension and tissue damage attributable to mineralocorticoid and high-salt diet, we evaluated the Th17/Treg response in DOCA–salt rats. The role of MR activation was analyzed, adding spironolactone or an antihypertensive therapy that was independent of the renin–angiotensin–aldosterone axis. Finally, the role of IL-17 in hypertension and tissue damage was studied in vivo by administration of specific anti–IL-17A antibodies to DOCA–salt rats.

Methods

Detailed description of all materials and methods used are provided in the online-only Data Supplement.

Results

DOCA–Salt Induces a Th17 Response That Is Blocked by Spironolactone

In the first protocol, we studied control, DOCA–salt, and DOCA–salt+spironolactone rats. DOCA–salt treatment increased systolic blood pressure (8–28 days) and heart and kidney weight and damaged kidney function (Table S1 in the online-only Data Supplement). All these effects were prevented by spironolactone treatment. To study Th17 activation in DOCA–salt rats, we measured RORγT (thymus-specific RAR-related orphan receptor gamma) mRNA, a transcription factor that promotes Th17 differentiation, in peripheral blood mononuclear cells (PBMCs). After DOCA–salt administration, RORγT mRNA abundance increased >300- and >200-fold at day 8 and 16 of treatment, respectively (Figure 1). We observed consistently an increase in IL-17 mRNA levels which correlated with the upregulation of IL-17 protein (Figure 1B and 1C). The treatment of DOCA–salt rats with spironolactone prevented the induction of RORγT, IL-17 mRNA, and IL-17 protein. Moreover, a significant increase of $CD4^+$/$IL\text{-}17^+$ cells was observed in PBMCs at day 8 of DOCA–salt treatment (Figure 1D), which was also blocked by spironolactone.

Next, we explored the role of secondary lymphoid organs in Th17 activation in DOCA–salt rats. At day 8 and 16 of DOCA–salt treatment, an increase in the abundance of RORγT mRNA was detected in the spleen (Figure S1A), associated with IL-17 mRNA and protein induction. Treating the DOCA–sat rats with spironolactone prevented upregulation of both RORγT and IL-17 (Figure S1A–S1C). Flow cytometry analysis of splenocytes revealed a marked increase of $CD4^+$/$IL\text{-}17^+$ cells in DOCA–salt rats, which was prevented by spironolactone (Figure S1D).

Consistent with the data showing Th17 response, we detected a significant upregulation of transcripts encoding cytokines that participate in the polarization/maintenance of a Th17 phenotype (TGF-β1, IL-1β, and IL-23p19; Figure S2A–S2F). In line with the findings described above, spironolactone treatment prevented all these changes.

Because recent studies in PBMCs of hypertensive patients showed increased cytotoxic $CD8^+$ T cells, therefore, we determined the presence of $CD8^+$/$IL\text{-}17^+$ T cells in PBMCs and splenocytes of hypertensive animals.[21] We observed increased $CD8^+$/$IL\text{-}17^+$ cells in DOCA–salt rats, an effect that was prevented by spironolactone (Figure S3).

DOCA–Salt Treatment Activates Th17 Response in Heart and Kidney

The heart from DOCA–salt rats at day 16 presented increased levels of TGF-β1 and IL-1β transcripts (Figure S4A and S4B); IL-23p19 mRNA was increased at day 8 and 16 (Figure S4C).

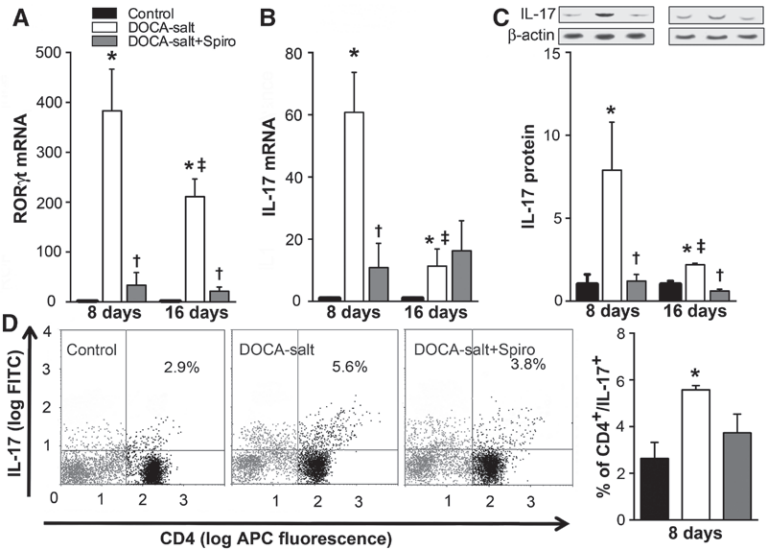

Figure 1. T-helper 17 lymphocyte (Th17) polarization in peripheral blood mononuclear cells (PBMCs) of deoxycorticosterone acetate and high-salt diet (DOCA–salt) rats is prevented by spironolactone. mRNA abundance of (**A**) RORγT (thymus-specific RAR-related orphan receptor gamma) and (**B**) interleukin-17A (IL-17A) measured by quantitative real-time polymerase chain reaction; *18S rRNA* was used as housekeeping gene. **C**, IL-17A protein abundance at day 8 and 16 of treatment, measured by Western blot. **Upper**, Representative immunoblots at day 8 and 16. **D**, Detection of $CD4^+$/$IL\text{-}17A^+$ cells by flow cytometry analysis in PBMCs at day 8 of treatment. Representative cytograms showing the percentage of $CD4^+$/$IL\text{-}17A^+$ and graph (**right**) summarizing the experiments. Data are expressed as mean±SEM (n=5). **P*<0.05 vs control; †*P*<0.05 vs DOCA–salt; ‡*P*<0.05 vs DOCA–salt, at day 8 of treatment. APC indicates allophycocyanin; and FITC, fluorescein isothiocyanate.

Spironolactone prevented or ameliorated the increase of TGF-β1, IL-1β, and IL-23p19 mRNAs. IL-17 mRNA abundance increased in hearts of DOCA–salt rats at day 16 (Figure 2A), correlating with IL-17A protein upregulation (Figure 2B).

Similarly, DOCA–salt treatment induced a marked increase in the abundance of TGF-β1, IL-1β, and IL-23p19 mRNA in kidney. However, the increase of Th17 polarizing cytokines was already significant after 8 days of DOCA–salt treatment (Figure S4D–S4F). Also, the induction of renal IL-17 mRNA and protein was already significant at day 8, reaching levels >20-fold higher than control at day 16 (Figure 2C). Spironolactone prevented the upregulation of TGF-β1, IL-1β, IL-23p19, and IL-17 mRNAs and IL-17 protein in kidney of DOCA–salt rats (Figure 2D).

Immunohistochemical studies showed perivascular infiltration of $CD4^+$ and $IL\text{-}17^+$ cells at day 16 in the heart of DOCA–salt rats (Figure S5A). In kidney, DOCA–salt treatment induced glomerular infiltration of $IL\text{-}17^+$ and $CD4^+$ cells at day 8 (Figure S5B). After 16 days, infiltrates were mainly detected in the peritubular space (Figure S5C). Spironolactone treatment prevented the infiltration of $CD4^+$ and $IL\text{-}17^+$ cells in heart and kidney.

Spironolactone Prevents Forkhead Box P3 and Tregs Reduction in DOCA–Salt Rats

Differentiation of Treg depends on the expression of forkhead box P3 (Foxp3) transcription factor.[16,17] DOCA–salt treatment decreased Foxp3 mRNA abundance in PBMCs at day 8 and 16. Of note, spironolactone treatment of DOCA–salt rats prevented the downregulation Foxp3 mRNA (Figure 3B). Flow cytometry analysis of PBMCs confirmed an increase of $Foxp3^+/CD4^+$ cells in PBMCs at day 8 (Figure 3A). In the spleen, spironolactone treatment of DOCA–salt rats increased Foxp3 mRNA (Figure S6A–S6C). Correspondingly, DOCA–salt treatment decreased Foxp3 mRNA in the kidney after 8 and 16 days of treatment (Figure 3D). Spironolactone treatment of DOCA–salt rats increased Foxp3 transcript at day 8 and 16 in both the heart and kidney (Figure 3C and 3D).

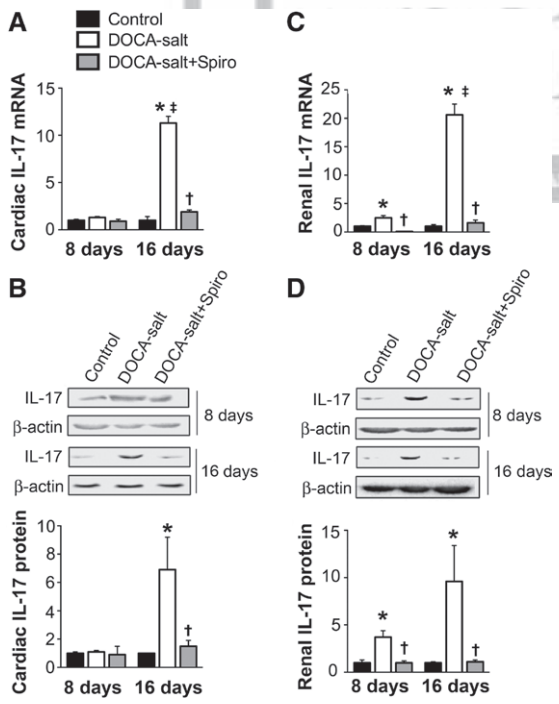

Figure 2. Spironolactone prevents interleukin-17 (IL-17) upregulation in heart and kidney of deoxycorticosterone acetate and high-salt diet (DOCA–salt) rats. IL-17 mRNA (**A**) and protein abundance (**B**) in heart. IL-17 mRNA (**C**) and protein abundance (**D**) in kidney. Transcripts were measured by quantitative real-time polymerase chain reaction; *18S rRNA* was used as housekeeping gene. Data are expressed as mean±SEM (n=5) **P*<0.05 vs control; †*P*<0.05 vs DOCA–salt; ‡*P*<0.05 vs DOCA–salt, at day 8 of treatment.

Antihypertensive Triple Therapy Does Not Abrogate the Th17 Response in DOCA–Salt Rats

To evaluate the contribution of hypertension per se versus MR activation in the Th17 response, antihypertensive triple therapy (reserpine+hydralazine+hydrochlorothiazide) was used. Triple therapy prevented hypertension in DOCA–salt rats (Table S2) and decrease in creatinine clearance, kidney hypertrophy, and proteinuria (Table S2). However, the increase of IL-17 and IL-23p19 transcripts in heart and kidney of DOCA–salt rats was not prevented by antihypertensive therapy (Figure 4). Fibrosis was not evident in the heart or kidney of DOCA–salt rats at 16 days (Figure S7).

Systemic Blockade of IL-17 Ameliorates Hypertension and Target Organ Damage Caused by DOCA–Salt Treatment

The effectiveness of IL-17 blockade for reversal of heart and kidney damage in DOCA–salt rats was evaluated. Uninephrectomized rats received DOCA–salt or vehicle for 16 days. Thereafter, DOCA–salt treated rats were randomly separated into 3 groups: anti–IL-17A IgG, isotype control IgG2b, and vehicle groups. The 4 experimental groups continued vehicle or DOCA–salt treatment ≤28 days. The administration of anti–IL-17A ameliorated hypertension in DOCA–salt rats after day 18. DOCA–salt rats that received the control nonspecific IgG2b exhibited hypertension similar to the DOCA–salt group (Figures 5A and S8).

DOCA–salt treatment increased TGF-β1, osteopontin (OPN), and NADPH oxidase-2 (NOX-2) transcripts (Figure 5B–5D). Similarly, DOCA–salt treatment increased collagen 1A (Col1A), connective tissue growth factor (CTGF), monocyte chemoattractant protein-1 (MCP-1), CD4, and p22phox mRNA abundance in heart and kidney (Figure S9A–S9E). Anti–IL-17A reversed the increase of all proinflammatory and profibrotic mediators (Figures 5B–5D and S9). Finally, DOCA–salt treatment increased Col1A and collagen deposits, whereas anti–IL-17A ameliorated Col1A (Figure 6) and collagen deposits (Figure S10) in cardiac and renal tissues. The IgG2b control treatment did not modify collagen abundance in hearts or kidneys of DOCA–salt rats. Cardiac hypertrophy, renal hypertrophy, and glomerular dysfunction were not modified by anti–IL-17 in DOCA–salt rats (Table S3).

Discussion

Our results show that DOCA–salt treatment elevates RORγT and IL-17 expression in PBMCs, spleen, heart, and kidney of DOCA–salt rats. Moreover, IL-17 induction correlated with the upregulation of IL-17 polarizing/maintenance cytokines

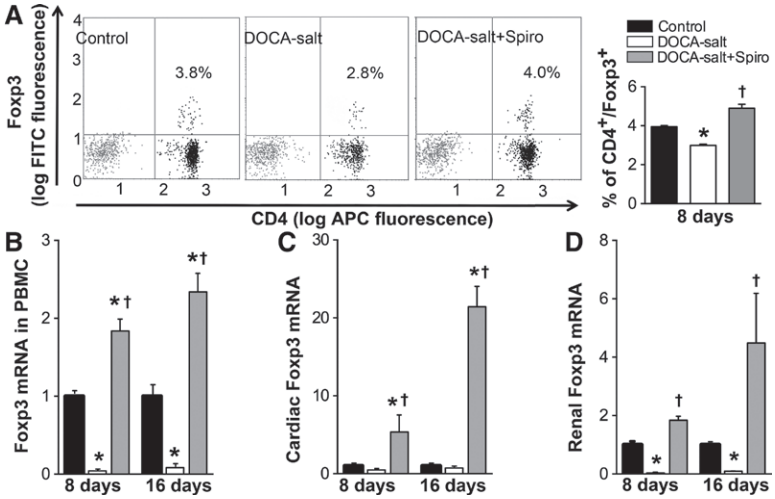

Figure 3. Forkhead box P3 (Foxp3) downregulation in peripheral blood mononuclear cells (PBMCs), heart, and kidney of deoxycorticosterone acetate and high-salt diet (DOCA–salt) rats. **A**, Flow cytometry analysis of $CD4^+/Foxp3^+$ cells in PBMCs, at 8 days of treatment. Representative cytograms with the percentage of $CD4^+/Foxp3^+$ cells are shown. Graph shows mean±SEM (n=7). Quantitative real-time polymerase chain reaction for Foxp3 mRNA in PBMCs (**B**), heart (**C**), and kidney (**D**) at day 8 and 16 of treatment. *18S rRNA* was used housekeeping gene. Data are expressed as mean±SEM (n=7). **P*<0.05 vs control; †*P*<0.05 vs DOCA–salt. APC indicates allophycocyanin; and FITC, fluorescein isothiocyanate.

(TGF-β1, IL-1β, and IL-23p19). All these changes were prevented by spironolactone. Thus, our results provide evidence of MR-dependent IL-17 activation in mineralocorticoid–high salt hypertension. The data are consistent with our previous in vitro studies, demonstrating that aldosterone-dependent MR activation potentiates the differentiation of $CD4^+$ T lymphocytes into Th17 cells.[22] The increase of $CD8^+/IL\text{-}17^+$ T cells in DOCA–salt rats suggest that Tc17 (cytotoxic T-lymphocyte-17) cells are implicated in mineralocorticoid–salt hypertension.

In the present study, we observed the increase of IL-17 polarizing cytokines and IL-17 in PBMCs and spleen, followed by heart and kidney. The rise of IL-17 in PBMCs and spleen was transient, decreasing concomitantly with the appearance of IL-17 in heart and kidney. These results suggest that antigens triggering the IL-17 response are first presented in lymphoid tissue[23] and that the ensuing appearance of IL-17 in cardiac and renal tissue may reflect the recruitment of T cells to sites of injury, as suggested by studies in cardiac and renal inflammatory diseases that involve Th17 response.[23–25]

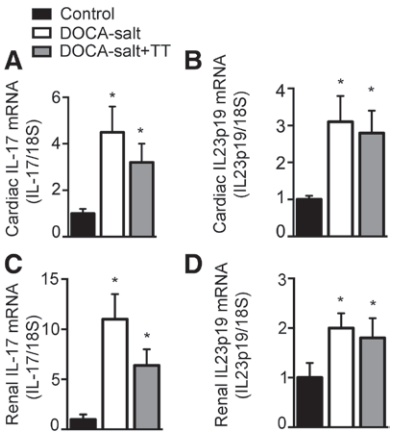

Figure 4. T-helper 17 lymphocyte (Th17) polarization in heart and kidney of deoxycorticosterone acetate and high-salt diet (DOCA–salt) rats treated with antihypertensive triple therapy (TT). Quantitative real-time polymerase chain reaction for (**A** and **C**) interleukin-17 (IL-17) and (**B** and **D**) IL-23 (p19 subunit) in heart (**A** and **B**) and kidney (**C** and **D**) at 16 days of treatment. *18S rRNA* was used as housekeeping gene. Data are expressed as mean±SEM (n=4). **P*<0.05 vs control.

In a second set of experiments in which DOCA–salt rats received antihypertensive therapy, we observed increased IL-17 mRNA abundance in heart and kidney even when hypertension was prevented. Thus, MR activation is required to trigger the IL-17 response in DOCA–salt rats. Our previous studies demonstrated that the blockade of the MR blunts the ability of aldosterone to induce Th17 polarization in vitro[22] and MR blockade reduced myocardial fibrosis and enhanced survival of mice with viral myocarditis, a Th17-associated disease.[26,27] Even though IL-17 blockade (protocol 3) ameliorated hypertension, oxidative stress, and fibrosis, we observed that the antihypertensive triple therapy prevented glomerular damage and cardiac hypertrophy in DOCA–salt rats, indicating

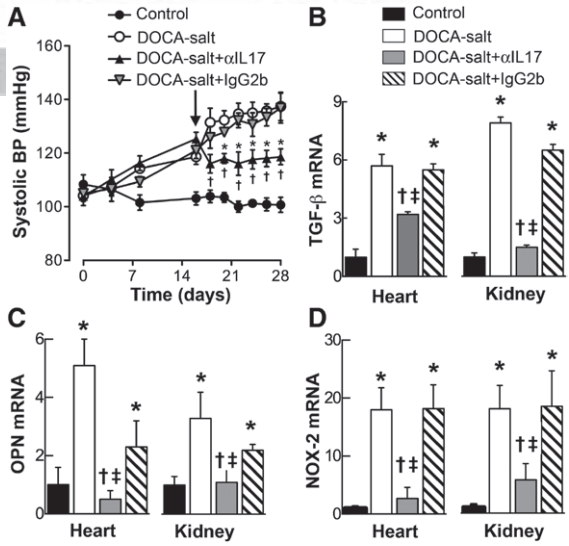

Figure 5. Systemic blockade of interleukin-17A (IL-17A) in deoxycorticosterone acetate and high-salt diet (DOCA–salt) rats. **A**, Systolic blood pressure (BP) during 28 days of study. Arrow indicates the beginning of treatment of DOCA–salt groups with anti–IL-17A or control IgG2b (each 2 days). Quantitative real-time polymerase chain reaction in heart and kidney for (**B**) transforming growth factor-β1 (TGF-β1), (**C**) osteopontin (OPN), and (**D**) NADPH oxidase-2 (NOX-2) at day 28 of treatment. *18S rRNA* was used as housekeeping gene. Data are expressed as mean±SEM (n=8). **P*<0.05 vs control; †*P*<0.05 vs DOCA–salt; ‡*P*<0.05 vs DOCA–salt+IgG2b.

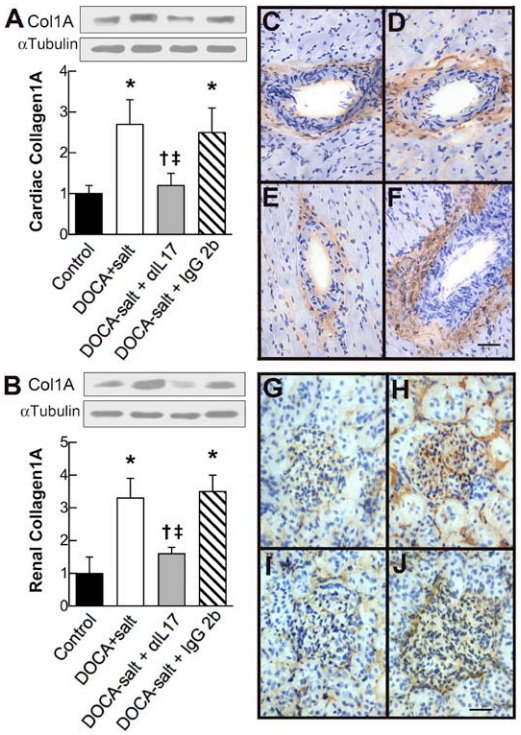

Figure 6. Relative abundance of collagen 1A (Col1A) in heart and kidney of deoxycorticosterone acetate and high-salt diet (DOCA–salt) rats treated with anti–interleukin-17A (IL-17A). Col1A protein abundance by Western blot in heart (**A**) and kidney (**B**). Data are expressed as mean±SEM (n=5). **P*<0.05 vs control; †*P*<0.05 vs DOCA–salt; ‡*P*<0.05 vs DOCA–salt+IgG2b. Immunohistochemistry for Col1A in heart (28 days) of control (**C**), DOCA–salt (**D**), DOCA–salt+anti–IL-17 (**E**), and DOCA–salt+IgG2b (**F**) rats. Immunohistochemistry for Col1A in kidney (28 days) of control (**G**), DOCA–salt (**H**), DOCA–salt+anti–IL-17 (**I**), and DOCA–salt+IgG2b (**J**) rats. Bar=30 μm (**F** and **J**).

that development of renal dysfunction and cardiac hypertrophy are blood pressure dependent.

The induction of Foxp3 expression in T cells results in a strong reduction of Th17 polarization and blunts the RORγt-induced expression of IL-17 both in vitro and in vivo.[16,17] We observed that concomitant with the IL-17 response, DOCA–salt rats exhibit significant decrease of Foxp3 mRNA and a reduction in $CD4^+/Foxp3^+$ cells in blood and splenocytes. Also, DOCA–salt+spironolactone rats presented increased $CD4^+/Foxp3^+$ cells in PBMCs and spleen and high levels of Foxp3 mRNA in heart and kidney. These results suggest that one of the deleterious effects of MR activation is the suppression of the Treg function. Recent studies have shown that Ang II–infused mice have decreased Treg[18] and that the adoptive transfer of Tregs in mice treated with aldosterone and salt prevents macrophage and T-cell infiltration in aorta and kidney.[20] Also, adoptive transfer of Tregs to Ang II mice ameliorated hypertension and arterial remodeling and increased NADPH oxidase activity in aorta, kidney, and heart.[18]

To test for a specific contribution of IL-17 to the phenotype of DOCA–salt rats, we examined the effects of specific anti–IL-17A antibodies administered to DOCA–salt rats with well-established hypertension, upregulation of IL-17 expression, and induction of the profibrotic mediator TGF-β1. We observed that anti–IL-17A IgG ameliorated hypertension and normalized the expression of NOX-2 and p22phox in heart and kidney, even in the context of mild hypertension. High levels of aldosterone and MR activation stimulate reactive oxygen species production in the kidney, cardiovascular system, and PBMCs.[28,29] Previous studies have also shown that aldosterone-salt treatment in rats increases NADPH oxidase activity and expression of p22phox and NOX-2, and the increase in reactive oxygen species production correlates with inflammation.[1,2,30] In addition, the incubation of vascular smooth muscle cells in the presence of IL-17 promotes reactive oxygen species generation, an effect that can be blocked by small interfering RNA targeting of NOX-2 or apocynin, an NADPH oxidase inhibitor.[31] Thus, we propose that the MR-dependent induction of IL-17 may contribute to oxidative stress in heart and kidney of DOCA–salt rats.

The use of antibodies to block IL-17A in vivo has some limitations. In the present study, we used the anti–IL-17 (R&D clone-41809; 100 μg/IP on alternate days), based on the previous study by Feng et al.[12] However, Markó et al[32] observed that anti–IL-17A (BD Biosciences, clone-18h10, 200 μg/IP, twice) did not reduce cardiac hypertrophy, fibrosis, or electric remodeling attributable to Ang II infusion, despite mildly reduced inflammation. These discrepant results suggest differences in the neutralizing activity of the antibodies and the half-life of IgGs, which may vary in the range of 24 to 80 hours, depending on particular clones.

It is recognized that MR-dependent fibrosis involves Col1A and CTGF upregulation.[1,2,30,33] In the present study, we observed that IL-17 antibody treatment ameliorated the increase of CTGF and collagen in cardiac and renal tissues. These results are consistent with the notion that IL-17 is a cytokine mediating MR-dependent induction of fibrosis in heart and kidney. In vivo studies have shown that IL-17 is a profibrotic cytokine in experimental autoimmune myocarditis and that it is critical for cardiac remodeling and progression to dilated cardiomyopathy.[11,34] The knockdown of IL-17R reduces Col1A expression, concentration, and cross-linking in hearts of spontaneously hypertensive rats.[13] Recent in vitro studies have shown that IL-17 directly induces proliferation and migration of mouse cardiac fibroblasts via Akt/microRNA-101/MAP kinase phosphatase-1 (MKP-1)–dependent p38 mitogen-activated protein kinase (MAPK) and extracellular signal-regulated kinase 1/2 (ERK1/2) activation[35] and that it induces MCP-1 release from cultured mouse mesangial cells via MAPK-ERK1/2 and p38 pathways.[36] We also observed that the treatment of DOCA–salt rats with anti–IL-17 antibody prevented OPN upregulation. These results suggest that the MR-dependent induction of MCP-1, macrophage infiltration, and the release of OPN by activated macrophages[37] are dependent on IL-17. Recent studies showed that the serum- and glucocorticoid-induced protein kinase 1 (SGK1) potentiates Th17 polarization because of high salt, and SGK1 has been proposed as a molecular mechanism by which a high-salt diet may trigger Th17 development and promote tissue inflammation.[38,39] Considering that *SGK1* is a rapid response gene for the MR, our results suggest that the reduction of Th17 response by spironolactone may imply a decrease in SGK1 activity. Further studies are needed to test this hypothesis directly and the molecular events involved.

In summary, we demonstrated that MR activation promotes Th17 polarization, which begins in PBMCs and spleen,

followed by polarization in heart and kidney. The Th17 polarization caused by MR activation correlates with decreased abundance of Treg cells. Blockade of IL-17 ameliorated hypertension and tissue fibrosis caused by DOCA–salt.

Perspectives

Our results show that IL-17 is implicated in high blood pressure and renal and myocardial fibrosis in mineralocorticoid–salt hypertension, expanding the role of IL-17 as a profibrotic cytokine in these tissues. Additional studies will be needed to determine the molecular mechanisms by which activation of MR modulates the immune response and the role of IL-17 in the development and progression of hypertension and tissue fibrosis. The data presented suggest that inhibition of IL-17 synthesis with the use of MR antagonists may be therapeutically useful to reduce blood pressure and tissue fibrosis in target organs. Further studies will be required to evaluate the potential of IL-17 blockade as a therapeutic strategy.

Acknowledgments

We thank Andrés Stutzin for critically revising this article.

Sources of Funding

This study was supported by the Millennium Institute on Immunology and Immunotherapy grant P09/016-F, CONICYT AT-24091044 to C.A. Amador, CONICYT Anillo ACT-71, CONICYT/FONDECYT/REGULAR/Nº1090223, Nº1130550, Fondecyt-FONDAP 15010006. C.A. Amador and A.A. Herrada were fellows of CONICYT. L. Carrasco was supported by CONICYT/FONDECYT/POSTDOCTORAL/ Nº grant 3060026.

Disclosures

None.

References

1. Brown NJ. Aldosterone and vascular inflammation. *Hypertension*. 2008;51:161–167.
2. Young MJ, Rickard AJ. Mechanisms of mineralocorticoid salt-induced hypertension and cardiac fibrosis. *Mol Cell Endocrinol*. 2012;350:248–255.
3. Svendsen UG. Evidence for an initial, thymus independent and a chronic, thymus dependent phase of DOCA and salt hypertension in mice. *Acta Pathol Microbiol Scand A*. 1976;84:523–528.
4. Olsen F. Transfer of arterial hypertension by splenic cells from DOCA-salt hypertensive and renal hypertensive rats to normotensive recipients. *Acta Pathol Microbiol Scand C*. 1980;88:1–5.
5. Guzik TJ, Hoch NE, Brown KA, McCann LA, Rahman A, Dikalov S, Goronzy J, Weyand C, Harrison DG. Role of the T cell in the genesis of angiotensin II induced hypertension and vascular dysfunction. *J Exp Med*. 2007;204:2449–2460.
6. Miossec P, Korn T, Kuchroo VK. Interleukin-17 and type 17 helper T cells. *N Engl J Med*. 2009;361:888–898.
7. Gaffen SL. Recent advances in the IL-17 cytokine family. *Curr Opin Immunol*. 2011;23:613–619.
8. Madhur MS, Funt SA, Li L, Vinh A, Chen W, Lob HE, Iwakura Y, Blinder Y, Rahman A, Quyyumi AA, Harrison DG. Role of interleukin 17 in inflammation, atherosclerosis, and vascular function in apolipoprotein e-deficient mice. *Arterioscler Thromb Vasc Biol*. 2011;31:1565–1572.
9. Eid RE, Rao DA, Zhou J, Lo SF, Ranjbaran H, Gallo A, Sokol SI, Pfau S, Pober JS, Tellides G. Interleukin-17 and interferon-gamma are produced concomitantly by human coronary artery-infiltrating T cells and act synergistically on vascular smooth muscle cells. *Circulation*. 2009;119:1424–1432.
10. Timmers L, Sluijter JP, van Keulen JK, Hoefer IE, Nederhoff MG, Goumans MJ, Doevendans PA, van Echteld CJ, Joles JA, Quax PH, Piek JJ, Pasterkamp G, de Kleijn DP. Toll-like receptor 4 mediates maladaptive left ventricular remodeling and impairs cardiac function after myocardial infarction. *Circ Res*. 2008;102:257–264.
11. Baldeviano GC, Barin JG, Talor MV, Srinivasan S, Bedja D, Zheng D, Gabrielson K, Iwakura Y, Rose NR, Cihakova D. Interleukin-17A is dispensable for myocarditis but essential for the progression to dilated cardiomyopathy. *Circ Res*. 2010;106:1646–1655.
12. Feng W, Li W, Liu W, Wang F, Li Y, Yan W. IL-17 induces myocardial fibrosis and enhances RANKL/OPG and MMP/TIMP signaling in isoproterenol-induced heart failure. *Exp Mol Pathol*. 2009;87:212–218.
13. Liu W, Wang X, Feng W, Li S, Tian W, Xu T, Song Y, Zhang Z. Lentivirus mediated IL-17R blockade improves diastolic cardiac function in spontaneously hypertensive rats. *Exp Mol Pathol*. 2011;91:362–367.
14. Madhur MS, Lob HE, McCann LA, Iwakura Y, Blinder Y, Guzik TJ, Harrison DG. Interleukin 17 promotes angiotensin II-induced hypertension and vascular dysfunction. *Hypertension*. 2010;55:500–507.
15. Vignali DA, Collison LW, Workman CJ. How regulatory T cells work. *Nat Rev Immunol*. 2008;8:523–532.
16. Ichiyama K, Yoshida H, Wakabayashi Y, Chinen T, Saeki K, Nakaya M, Takaesu G, Hori S, Yoshimura A, Kobayashi T. Foxp3 inhibits RORγt-mediated IL-17A mRNA transcription through direct interaction with RORγt. *J Biol Chem*. 2008;283:17003–17008.
17. Zhou L, Lopes JE, Chong MMW, Ivanov II, Min R, Victora GD, Shen Y, Du J, Rubtsov YP, Rudensky AY, Ziegler SF, Littman DR. TGF-β-induced Foxp3 inhibits TH17 cell differentiation by antagonizing RORγt function. *Nature*. 2008;453:236–240.
18. Barhoumi T, Kasal DA, Li MW, Shbat L, Laurant P, Neves MF, Paradis P, Schiffrin EL. T regulatory lymphocytes prevent angiotensin II-induced hypertension and vascular injury. *Hypertension*. 2011;57:469–476.
19. Kvakan H, Kleinewietfeld M, Qadri F, Park JK, Fischer R, Schwarz I, Rahn HP, Plehm R, Wellner M, Elitok S, Gratze P, Dechend R, Luft FC, Muller DN. Regulatory T cells ameliorate angiotensin II-induced cardiac damage. *Circulation*. 2009;119:2904–2912.
20. Kasal DA, Barhoumi T, Li MW, Yamamoto N, Zdanovich E, Rehman A, Neves MF, Laurant P, Paradis P, Schiffrin EL. T regulatory lymphocytes prevent aldosterone-induced vascular injury. *Hypertension*. 2012;59:324–330.
21. Youn JC, Yu HT, Lim BJ, Koh MJ, Lee J, Chang DY, Choi YS, Lee SH, Kang SM, Jang Y, Yoo OJ, Shin EC, Park S. Immunosenescent CD8+ T cells and C-X-C chemokine receptor type 3 chemokines are increased in human hypertension. *Hypertension*. 2013;62:126–133.
22. Herrada AA, Contreras FJ, Marini NP, Amador CA, González PA, Cortés CM, Riedel CA, Carvajal CA, Figueroa F, Michea LF, Fardella CE, Kalergis AM. Aldosterone promotes autoimmune damage by enhancing Th17-mediated immunity. *J Immunol.* 2010;184:191–202.
23. Herrada AA, Campino C, Amador CA, Michea LF, Fardella CE, Kalergis AM. Aldosterone as a modulator of immunity: implications in the organ damage. *J Hypertens.* 2011;29:1684–1692.
24. Frangogiannis NG. Regulation of the inflammatory response in cardiac repair. *Circ Res*. 2012;110:159–173.
25. Yang M, Deng J, Liu Y, Ko KH, Wang X, Jiao Z, Wang S, Hua Z, Sun L, Srivastava G, Lau CS, Cao X, Lu L. IL-10-producing regulatory B10 cells ameliorate collagen-induced arthritis via suppressing Th17 cell generation. *Am J Pathol*. 2012;180:2375–2385.
26. Yuan J, Cao AL, Yu M, Lin QW, Yu X, Zhang JH, Wang M, Guo HP, Liao YH. Th17 cells facilitate the humoral immune response in patients with acute viral myocarditis. *J Clin Immunol*. 2010;30:226–234.
27. Xiao J, Shimada M, Liu W, Hu D, Matsumori A. Anti-inflammatory effects of eplerenone on viral myocarditis. *Eur J Heart Fail*. 2009;11:349–353.
28. Nishiyama A, Yao L, Nagai Y, Miyata K, Yoshizumi M, Kagami S, Kondo S, Kiyomoto H, Shokoji T, Kimura S, Kohno M, Abe Y. Possible contributions of reactive oxygen species and mitogen-activated protein kinase to renal injury in aldosterone/salt-induced hypertensive rats. *Hypertension*. 2004;43:841–848.
29. Ahokas RA, Warrington KJ, Gerling IC, Sun Y, Wodi LA, Herring PA, Lu L, Bhattacharya SK, Postlethwaite AE, Weber KT. Aldosteronism and peripheral blood mononuclear cell activation: a neuroendocrine-immune interface. *Circ Res*. 2003;93:e124–e135.
30. Briet M, Schiffrin EL. Aldosterone: effects on the kidney and cardiovascular system. *Nat Rev Nephrol*. 2010;6:261–273.
31. Pietrowski E, Bender B, Huppert J, White R, Luhmann HJ, Kuhlmann CR. Pro-inflammatory effects of interleukin-17A on vascular smooth muscle cells involve NAD(P)H- oxidase derived reactive oxygen species. *J Vasc Res*. 2011;48:52–58.
32. Markó L, Kvakan H, Park JK, Qadri F, Spallek B, Binger KJ, Bowman EP, Kleinewietfeld M, Fokuhl V, Dechend R, Müller DN. Interferon-γ signaling inhibition ameliorates angiotensin II-induced cardiac damage. *Hypertension*. 2012;60:1430–1436.

33. Brem AS, Morris DJ, Gong R. Aldosterone-induced fibrosis in the kidney: questions and controversies. *Am J Kidney Dis*. 2011;58:471–479.
34. Liu Y, Zhu H, Su Z, Sun C, Yin J, Yuan H, Sandoghchian S, Jiao Z, Wang S, Xu H. IL-17 contributes to cardiac fibrosis following experimental autoimmune myocarditis by a PKCβ/Erk1/2/NF-κB-dependent signaling pathway. *Int Immunol*. 2012;24:605–612.
35. Valente AJ, Yoshida T, Gardner JD, Somanna N, Delafontaine P, Chandrasekar B. Interleukin-17A stimulates cardiac fibroblast proliferation and migration via negative regulation of the dual-specificity phosphatase MKP-1/DUSP-1. *Cell Signal*. 2012;24:560–568.
36. Iyoda M, Shibata T, Kawaguchi M, Hizawa N, Yamaoka T, Kokubu F, Akizawa T. IL-17A and IL-17F stimulate chemokines via MAPK pathways (ERK1/2 and p38 but not JNK) in mouse cultured mesangial cells: synergy with TNF-alpha and IL-1beta. *Am J Physiol Renal Physiol*. 2010;298:F779–F787.
37. Azibani F, Benard L, Schlossarek S, Merval R, Tournoux F, Fazal L, Polidano E, Launay JM, Carrier L, Chatziantoniou C, Samuel JL, Delcayre C. Aldosterone inhibits antifibrotic factors in mouse hypertensive heart. *Hypertension*. 2012;59:1179–1187.
38. Kleinewietfeld M, Manzel A, Titze J, Kvakan H, Yosef N, Linker RA, Muller DN, Hafler DA. Sodium chloride drives autoimmune disease by the induction of pathogenic TH17 cells. *Nature*. 2013;496:518–522.
39. Wu C, Yosef N, Thalhamer T, Zhu C, Xiao S, Kishi Y, Regev A, Kuchroo VK. Induction of pathogenic TH17 cells by inducible salt-sensing kinase SGK1. *Nature*. 2013;496:513–517.

Novelty and Significance

What Is New?

- Deoxycorticosterone acetate and high-salt diet rats present T-helper 17 lymphocyte response and regulatory T-lymphocyte downregulation. T-helper 17 lymphocyte/regulatory T-lymphocyte imbalance is dependent on mineralocorticoid receptor activation and can be prevented by spironolactone.
- The blockade of interleukin-17 in the context of high-salt diet and mineralocorticoid excess ameliorates hypertension, NADPH induction, and cardiac and renal fibrosis.

What Is Relevant?

- These findings show that inappropriate mineralocorticoid receptor activation in the context of high-salt diet is pathogenic through T-helper 17 lymphocyte/regulatory T-lymphocyte imbalance.
- Spironolactone prevents this adaptive immune response and tissue fibrosis, and interleukin-17 may be a new therapeutic target for the treatment of tissue damage in hypertension.

Summary

T-helper 17 lymphocyte/regulatory T-lymphocyte imbalance is a key contributor to hypertension and cardiac and renal damage in mineralocorticoid+high-salt–dependent hypertension that may be ameliorated/prevented by mineralocorticoid receptor pharmacological blockade and interleukin-17 blockade.

Hypertension
Journal of the American Heart Association

Spironolactone decreases DOCA-salt induced organ damage by blocking the activation of T helper 17 and the downregulation of regulatory T lymphocytes

Cristián A. Amador[1,2]*, Víctor Barrientos[1,2]*, Juan Peña[1,2], Andrés A. Herrada[3], Magdalena González[1,2], Solange Valdés[1,2], Loreto Carrasco[1], Rodrigo Alzamora[1,2], Fernando Figueroa[4], Alexis M. Kalergis[3] and Luis Michea[1,2]

[1]Center for Molecular Studies of the Cell; [2]Millennium Institute on Immunology and Immunotherapy, ICBM, Facultad de Medicina, Universidad de Chile; [3]Millennium Institute on Immunology and Immunotherapy, Departamento de Genética Molecular y Microbiología, Facultad de Ciencias Biológicas and Departamento de Reumatología, Facultad de Medicina, Pontificia Universidad Católica de Chile; [4]Facultad de Medicina, Universidad de los Andes, Santiago, Chile.

*C.A.A and V.B. are joint first authors

Short title: DOCA-Salt induces fibrosis via Th17

Address correspondence to:

Dr. Luis F. Michea

Facultad de Medicina, Universidad de Chile

Ave. Independencia 1027

Santiago, Chile

Tel: 56-2-9786993 / Fax: 56-2-29786494

E-mail: lmichea@med.uchile.cl

SUPPLEMENTAL MATERIAL

I. Material and Methods

Animals and Experimental Protocol

We performed three separate sets of experiments: In Protocol 1, we evaluated the time course of IL-17 induction and the role of MR activity in the induction of Th17 immune response. In Protocol 2, we analyzed the role of high blood pressure *vs* MR activation as inducers of Th17 response in DOCA-salt rats. In Protocol 3, we studied the effect of systemic IL-17 blockade in hypertension proinflammatory and profibrotic mediators in DOCA-salt rats. The Ethics Committee of the Universidad de Chile approved the protocols for animal experimentation according to the National Institutes of Health Guide for the Care and Use of Laboratory Animals.

We used male Sprague-Dawley rats (150-180 g). The animals were uninephrectomized under ketamine/xylazine anesthesia (90 mg/kg and 10 mg/kg IP, respectively). After 1 week of surgery, the rats were randomized to different groups according the experimental protocol, as described below (n=5 to 8 in each group; 120 animals total).

Protocol 1: Time course of Th17 response and role of MR activity

Uninephrectomized rats were separated in three groups: (1) Control (vehicle, free access to tap water), (2) Deoxycorticosterone acetate (DOCA)-salt (30 mg/kg + 0.9% NaCl/0.3% KCl in drinking water) (Sigma-Aldrich, St. Louis, MO, USA), and (3) DOCA-salt plus Spironolactone (50 mg/kg, DOCA-salt + Spiro) (Laboratorio Chile). DOCA was dissolved in olive oil and given by intramuscular injection twice a week. Spiro was administered in the food.[29] These experimental groups were studied at 8, 16 and 28 days.

Protocol 2: Role of hypertension *vs* MR activation as inducers of Th17

Uninephrectomized rats were treated for 16 days with DOCA-salt and separated into two groups: (1) DOCA-salt, and (2) DOCA-salt plus Anti-hypertensive Triple Therapy (0.32 mg/kg Reserpine, 6.5 mg/kg Hydralazine, 4 mg/kg Hydrochlorothiazide), added to the saline drinking water. A third group of uninephrectomized rats receiving vehicle injection with free access to water (no salt added) was the paired control group in this protocol.

Protocol 3: Effect of systemic blockade of IL-17A in hypertension, proinflammatory and profibrotic mediators

The uninephrectomized rats received DOCA-salt treatment for 16 days. Then, the animals were randomly separated into three groups: (1) DOCA-salt, (2) DOCA-salt plus anti-IL-17A antibody (100 µg/day, clone: 41809), and (3) DOCA-salt plus IgG2b (100 µg/day, clone 20116) (R&D Systems, Minneapolis, MN, USA), as isotype control. Anti-IL-17A, IgG2b or PBS 1X were injected intraperitoneally, every 2 days (six times in all). A fourth group of rats (control, paired) received intramuscular vehicle injections. The total duration of this protocol was 28 days.

Physiological studies

One week before surgery the rats were trained for systolic blood pressure measurements by the tail-cuff method (PowerLab Chart, ADInstrument, Dunedin, New Zealand).[29] Two days after surgery, the measurements of blood pressure by the tail-cuff method started again, to keep the animals trained. The data of blood pressure that we present were obtained 8 days after starting the protocols. 48 hours before finishing each experimental period, all rats were housed in metabolic cages. Samples obtained during the last 24 hours were used for urine output measurements and biochemical analysis. After urine

recollection the rats were euthanized to obtain blood and tissue samples. Aliquots of plasma and urine were assayed for creatinine using automated chemistry (Jaffe Assay). The creatinine clearance was calculated according to the standard formula. Urinary protein was measured using Bradford Reagent, Sigma-Aldrich® (St. Louis, MO, USA).[29] Plasma was separated by centrifugation (3000 rpm for 5 min at 4ºC). Heart and kidney were quickly removed, weighed. 50% of the isolated tissue was used to isolate total RNA and to prepare total protein homogenates. The remaining tissue samples were used for immunohistochemical analysis.

Total RNA isolation and real-time semiquantitative RT-PCR

Total RNA from heart and kidney samples was extracted with TRIzol (Invitrogen, Carlsbad, CA, USA), according to manufacturer's instructions. After checking the RNA quality (agarose gel electrophoresis)[30], we used aliquots of 250 ng as template for reverse-transcription (random hexamers, Improm II Reverse Transcriptase System; Promega, Madison, WI, USA). cDNAs were amplified with 2 U of TaqDNA polymerase (Promega,) and detected by SYBRGreen method (Molecular Probes-Invitrogen). Non-transcribed total RNA was used as negative control (to detect genomic DNA contamination). All real-time PCR reactions were performed using a Stratagene thermal cycler (model Mx300P). PCR amplification of the 18S ribosomal RNA served as internal control. In the preliminary studies, PCR products were subjected to agarose gel electrophoresis and melting curve program to confirm amplification specificity.

The sequences of the primer pairs used for cDNA quantitation are as follows:

Col1A forward (F), 5`-TGCTGCCTTTTCTGTTCCTT-3`
reverse (R), 5`-AAGGTGCTGGGTAGGGAAGT-3`

CTGF forward (F), 5`-AGCTTGCTTGCAGACAGACCT-3`
reverse (R), 5`-TCACTTGCCACAAGCTGTCCA-3`

Foxp3 forward (F), 5`-AGGCACTTCTCCAGGACAGA-3`
reverse (R), 5`-CTGGACACCCATTCCAGACT-3`

IL-17A forward (F), 5`-CTTCACCTTGGACTCTGAGC-3`
reverse (R), 5`-TGGCGGACAATAGAGGAAAC-3`

IL-1β forward (F), 5`-CTGTGACTCGTGGGATGATG-3`
reverse (R), 5`-GGGATTTTGTCGTTGCTTGT-3`

IL-23p19 forward (F), 5`-CAGGTTCCCATGGCTACAGT-3`
reverse (R), 5`-TCTGGGGTTTGTTGCTTTTC-3`

MCP-1 forward (F), 5`-GATGCAGTTAATGCCCCACT-3`
reverse (R), 5`-TTCCTTATTGGGGTCAGCAC-3`

NOX-2 forward (F), 5`-CTGGGCACTCCTTTATTTTTC-3`
reverse (R), 5`-CCATTCGGAGGTCTTACTTTG-3`

OPN forward (F), 5`-GAGGAGAAGGCGCATTACAG-3`
reverse (R), 5`-ATGGCTTTCATTGGAGTTGC-3`

RORγT forward (F), 5`- GCCTACAATGCCAACAACCACACA -3`
reverse (R), 5`-TGATGAGAACCAAGGCCGTGTAGA -3`

TGF-β1 forward (F), 5`-GACCTGCTGGCAATAGCTTC-3`
reverse (R), 5`-GGGTCTCCCAAGGAAAGGTA-3`

p22phox forward (F), 5´-CCC CCG GGG AAA GAG GAA AA-3´
reverse (R), 5´-GCA GGC GAC AGC ACT AAG-3´

p47phox forward (F), 5´-GGC CAA AGA TGG CAA GAA TA-3´
reverse (R), 5´-TGT CAA GGG GCT CCA AAT AG -3´

NOX4 forward (F), 5´-ACCAGATGTTGGGCCTAGGATTGT-3´
reverse (R), 5´-AGTTCACTGAGAAGTTCAGGGCGT-3´

CD4 forward (F), 5´-TCT TCC CAG TCC TGG ATC AC-3´
reverse (R), 5´-CAC CAC CAGGTT CACTTC CT-3´

After setting the PCR protocol and confirm the identity of products, all PCR products obtained in subsequent experiments were subjected to melting curve program to confirm amplification specificity. Results were analyzed according to the standard curve method (correlation coefficient ≥ 0.98)[30]. Specific mRNA abundance was calculated as the ratio of the specific mRNA amount relative to the amount of 18S for each sample, measured in duplicate. Results are expressed as relative abundance in arbitrary units.

Western Blot

For total protein extraction, the tissues were homogenized in ice-cold sucrose buffer (100 mmol/L Tris-HCl, 5 mmol/L $MgCl_2$, 250 mmol/L sucrose, pH=7.6). PBMC were isolated by density gradient centrifugation on Ficoll-Hypaque (Sigma-Aldrich, St. Louis, MO, USA). Total protein extract from PBMC was obtained by extraction in Laemlli buffer (200 µL). All samples (50 µg of protein) were incubated for 5 min at 95°C and separated by SDS-PAGE. After electrophoresis the proteins were electroblotted onto nitrocellulose membranes (Thermo-Scientific, Rockford, IL, USA), and probed with primary antibodies against IL-17A (rabbit polyclonal: H-132, catalog number: sc-7927) and Col1A (mouse monoclonal, catalog number: sc-59772). Then, blots were incubated 1hr at room temperature with secondary antibody anti-rabbit-HRP (Calbiochem-Millipore, Billerica, MA, USA), anti-mouse-HRP (Calbiochem-Millipore) or anti-goat-HRP (Santa Cruz Biotechnology, Santa Cruz, CA, USA) diluted 1:5000 in 5% non-fat milk TBST washed again with TBST (three times for 15 min). The levels of protein were normalized to the levels of β-Actin or α-Tubulin (1:2000, Santa Cruz Biotechnology). Specific binding was detected using enhanced chemiluminescence (Thermo-Scientific Pierce, Rockford, IL, USA) and exposed to CL-XPosure TM Film (Thermo-Scientific Pierce). Blots were quantified by densitometry analysis (Adobe Photoshop 7.0).[29,30]

Flow Cytometry

PBMC and cells collected from rat spleen, obtained with 70-µm sterile cell strainer (Becton Dickinson, San Jose, CA, USA), were incubated for 30 min at 4°C with APC anti-CD4 (1:200) (clone OX35, eBioscience, San Diego, CA, USA). For intracellular staining, cells were fixed in 4% paraformaldehyde for 10 min at 4°C. After washing, cells were

permeabilized (PBS 1X/BSA 3%/Saponin 0,5%) for 10 min and then incubated with FITC anti-IL-17A (1:200) (clone eBio17B7, eBioscience) and an Alexa Fluor® 488 anti-Foxp3 (1:200) (clone FJK-16s, eBioscience) for 1hr at 4°C. For IL-17A detection, cells were stimulated with PMA (10 ng/ml; Sigma-Aldrich), ionomycin (1 mg/ml; Calbiochem) and brefeldin A (5 mg/ml; Sigma-Aldrich) for 5 hr at 37ºC. Cells were analyzed in FACSCanto-II (Becton Dickinson). Fluorescence data from at least 20.000 events were collected for each sample. Analysis of data was performed using WinMDI software (downloaded from http://facs.scripps.edu).

Immunohistochemistry

For IL-17 and CD4, heart and kidney sections were fixed in 10% formalin and embedded in paraffin to prepare sections in a Leitz Wetzlar Manual Microtome Type 1212 (Wetzlar, Germany). For collagen immunodetection heart and kidney tissue sections were mounted in O.C.T embedding medium (Tissue-Tek™, Sakura Finetek, Torrance, CA, USA), snap frozen in supercooled isopentane and stored at -80°C, before cryosectioning (5-µm thick). Cryosections were methanol-fixed (overnight, -20ºC). Sections were washed with PBS 1X and incubated in 0.3% hydrogen peroxidase for 15 min at room temperature for blocking endogenous peroxidase activity, washed with PBS 1X and blocked with Serum Vectastain Elite ABC Kit (PK-6100 VectorLabs, Burlingame, CA, USA) for 15 min at room temperature and then incubated with IL-17A (1:500) (rabbit polyclonal: H-132, catalog number: sc-7927), CD4 (1:200) (mouse monoclonal: 5B5, catalog number: sc-70671) and Col1A (1:500) (mouse monoclonal, catalog number: sc-59772) (all from Santa Cruz Biotechnology) in Serum Vectastain Elite ABC Kit (PK-6100 VectorLabs, Burlingame, CA, USA) overnight at 4ºC. The sections were incubated with secondary antibodies Vectastain Elite ABC Kit for 20 min at 37ºC and washed with PBS 1X. Staining was completed after 3 min of incubation with freshly prepared ImmPACT™ DAB Peroxidase Substrate (SK-4105). Then the samples were washed with PBS 1X. For Masson's staining cardiac and kidney tissue were fixed in neutral-formalin and embedded in paraffin. Sections were prepared and stained with Masson's trichrome.

Data Presentation and Statistical Analysis

Results are expressed as mean±SEM. Data were analyzed by 2-tailed ANOVA analysis followed by Bonferroni *post hoc* tests. Values of $P<0.05$ were considered statistically significant.

II. Supplemental Tables

Table S1. Physiological Parameters of Control Rats, DOCA-Salt Rats, and DOCA-Salt plus Spironolactone Rats

	8 Days			16 Days			28 Days		
Parameter	**Control**	**DOCA-salt**	**DOCA-salt Spiro**	**Control**	**DOCA-salt**	**DOCA-salt Spiro**	**Control**	**DOCA-salt**	**DOCA-salt Spiro**
SBP (mmHg)	122±2.1	159±8.7*	126±6.3†	120±4.7	170±16*	117±4.0†	118±5.3	169±8.3*	115±3.8†
HW/BW (mg/g)	3.3±0.1	3.7±0.2	3.3±0.1	3.1±0.1	3.5±0.1*	3.3±0.1	3.0±0.1	3.8±0.1*	3.4±0.0†
KW/BW (mg/g)	5.2±0.1	5.9±0.4	5.1±0.1	5.1±0.0	6.3±0.0*	5.1±0.1†	5.2±0.1	6.4±0.2*	5.0±0.5†
Creatinine Clearance (mL/min)	2.2±0.1	1.1±0.2*	2.1±0.1†	2.1±0.3	1.3±0.3*	2.0±0.1†	2.2±0.3	0.5±0.1*	2.1±0.2†
Proteinuria (mg/day)	4.5±0.4	12.5±1.7*	4.5±0.8†	3.6±1.6	10.3±1.6*	3.0±0.6†	4.0±1.1	15.0±3.2*	3.0±0.7†

Abbreviations: SBP, systolic blood pressure; HW/BW, heart weight/body weight ratio; KW/BW, kidney weight/body weight ratio; Spiro, spironolactone. Statistically significant differences between groups are indicated. Data are expressed as average values ±SEM (n=7). *P<0.05 versus control; †P<0.05 versus DOCA-salt.

Table S2. Effect of Anti-hypertensive Therapy on Physiological Parameters of Control and DOCA-Salt Rats

Parameter	Control	DOCA-salt	DOCA-salt + Triple
SBP (mmHg)	104±0.9	163±8.0 *	114±1.6 †
HW/BW (mg/g)	3.8±0.3	4.2±0.3	4.0±0.1
KW/BW (mg/g)	5.9±0.5	8.1±0.1 *	6.3±0.3 †
Creatinine Clearance (mL/min)	2.1±0.0	1.1±0.3 *	3.1±0.4 †
Proteinuria (mg/d)	3.7±0.7	15.3±2.6 *	5.0±0.3 †

Physiological parameters of control (vehicle), DOCA-salt, and DOCA-salt treated with antihypertensive therapy ("Triple"). Statistically significant differences between DOCA-salt and DOCA-salt + Triple are indicated (n=6). *P < 0.05 versus value of control group; †P < 0.05 versus DOCA-salt. **Abbreviations**: SBP, systolic blood pressure; HW/BW, heart weight/body weight ratio; KW/BW, kidney weight/body weight.

Table S3. Physiological Parameters of Control, DOCA-Salt, DOCA-salt+Anti-IL-17 and DOCA-salt+IgG2b Rats

Parameter	Control	DOCA-salt	DOCA-salt+Anti-IL-17	DOCA-salt + IgG2b
HW/BW (mg/g)	4.2±0.3	5.4±0.2*	5.4±0.1*	5.7±0.3*
KW/BW (mg/g)	7.1±0.1	8.9±0.3*	8.3±0.3*	8.8±0.4*
Creatinine Clearance (mL/min)	1.9±0.1*	0.8±0.1*	0.8±0.1*	0.8±0.1*
Proteinuria (mg/d)	4.5±0.9*	14.5±1.0*	16.9±1.2*	15.9±2.1*

Physiological parameters of rats from control (vehicle), DOCA-salt, DOCA-salt+Anti-IL-17 IgG and DOCA-salt+IgG2b (control IgG) groups (28 days). *$P < 0.05$ versus value of control group, n=5-8 rats per group. **Abbreviations**: HW/BW, heart weight/body weight ratio; KW/BW, kidney weight/body weight.

III. Supplementary Figures

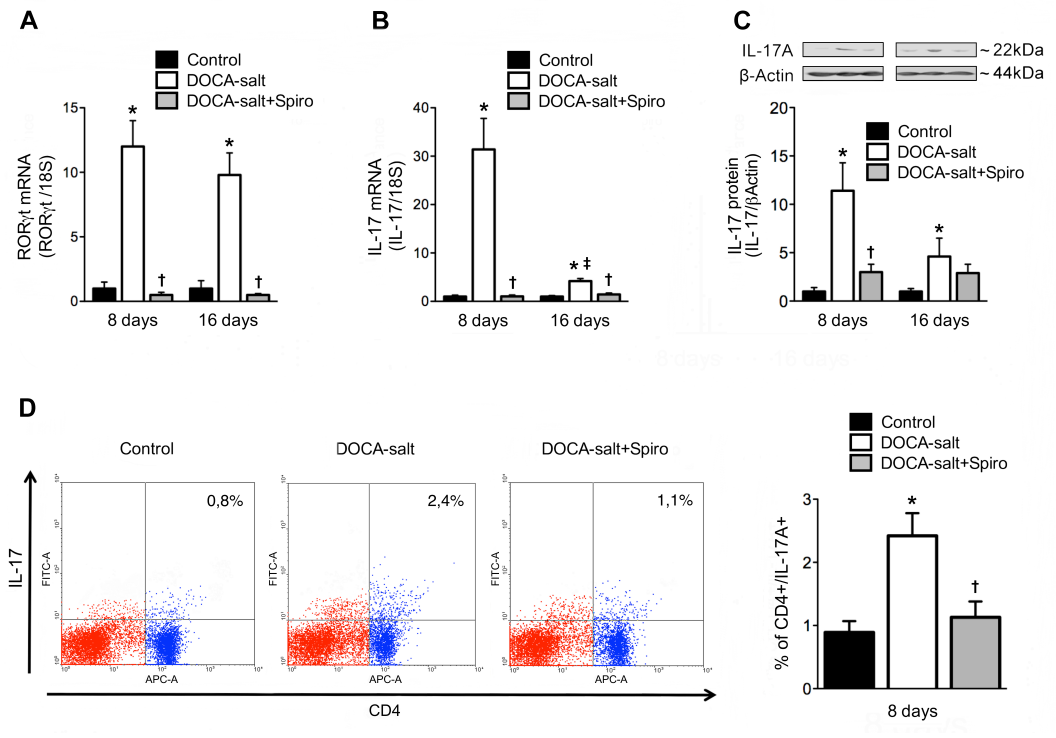

Figure S1. Th17 polarization in Splenocytes of DOCA-salt rats is prevented by spironolactone. (**A**) RORγT mRNA and (**B**) IL-17A mRNA abundance measured by qRT-PCR with specific primers; 18S rRNA was used to normalize abundance of mRNA. (**C**) IL-17A protein abundance at 8 and 16 days of treatment, measured by Western blot and using β-actin as loading control. (**D**) Detection of $CD4^+/IL\text{-}17A^+$ cells in splenocytes at 8 days of treatment by flow cytometry. Data are expressed as average values ± SEM (n=5) **P* < 0.05 versus value of control group; †*P* < 0.05 versus DOCA-salt group; ‡*P* < 0.05 versus DOCA-salt, at 8 days of treatment.

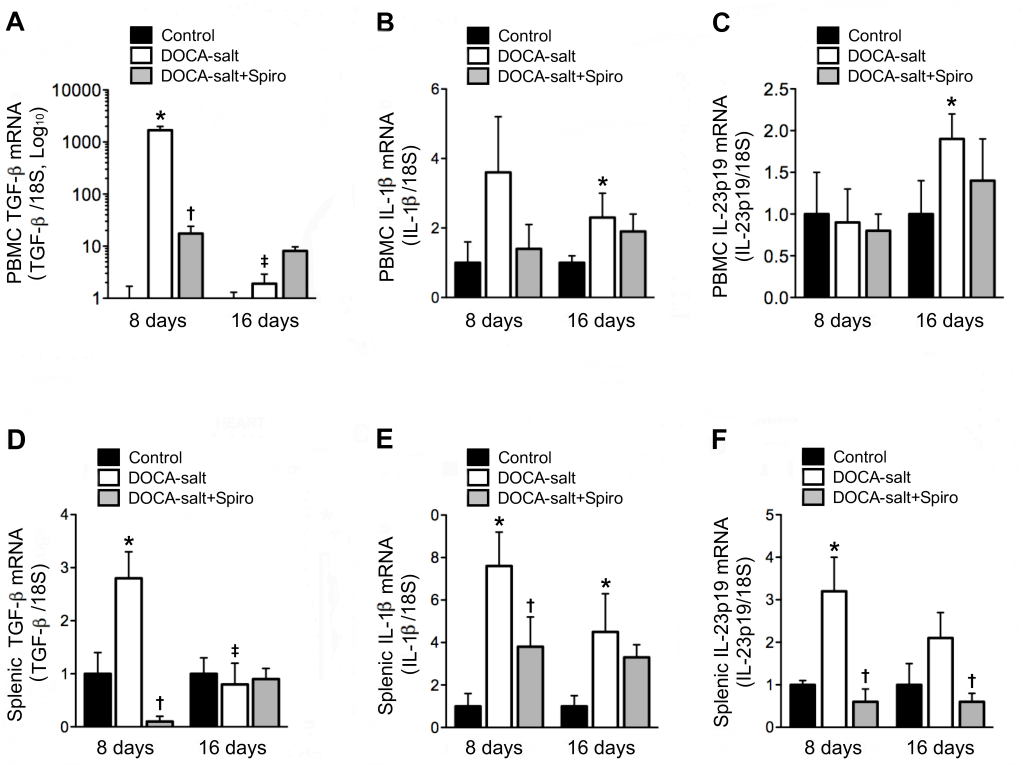

Figure S2. Spironolactone ameliorates induction of cytokines that promote/maintain Th17 polarization in PBMC and spleen of DOCA-salt rats. qRT-PCR for: (**A** and **D**) TGF-β1, (**B** and **E**) IL-1β, and (**C** and **F**) IL-23 (p19 subunit), in (**A–C**) PBMC and spleen (**D–F**) kidney at 8 and 16 days of treatment. 18S rRNA was used to normalize abundance of mRNA. Data are expressed as average values ± SEM (n=5) *P < 0.05 versus value of control group; †P < 0.05 versus DOCA-salt group; ‡P < 0.05 versus DOCA-salt, at 8 days of treatment.

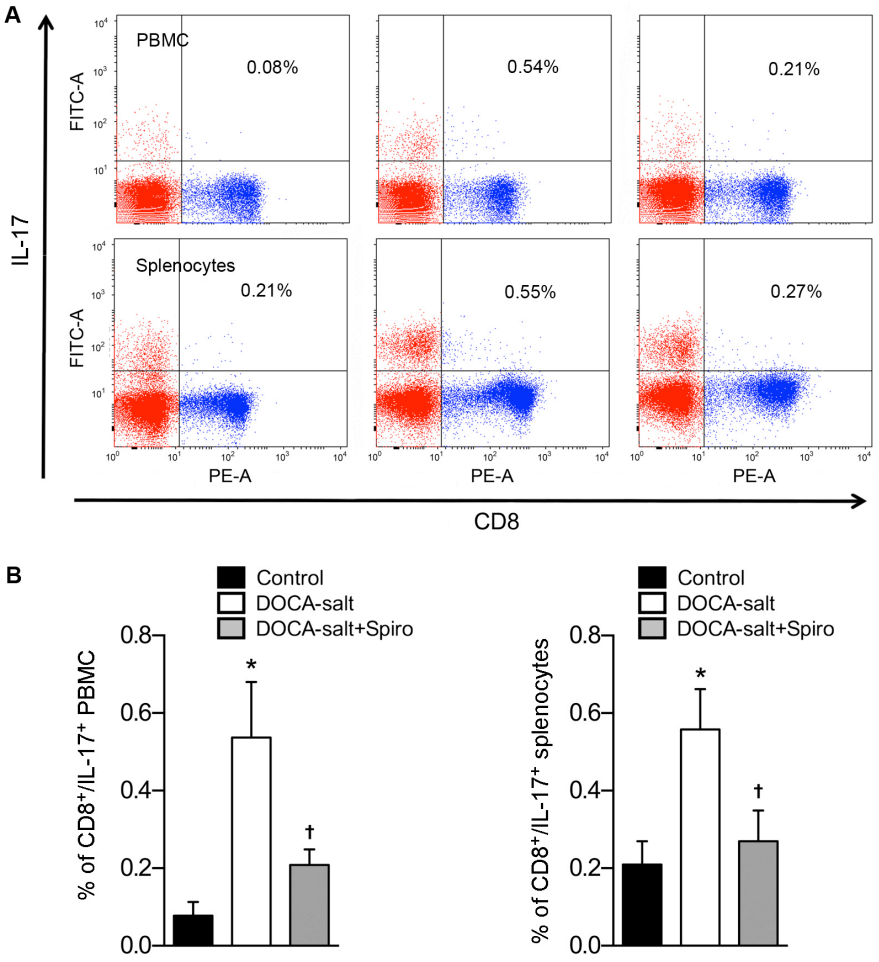

Figure S3. Increase of $CD8^+/IL17^+$ cells in PBMC and splenocytes of DOCA-salt rats is prevented by spironolactone. (**A**) Detection of $CD8^+/IL\text{-}17A^+$ cells in PBMC (upper panels) and splenocytes (lower panels) at 8 days of treatment by flow cytometry. (B) Bars represent average values ± SEM (n=5) **P* < 0.05 versus value of control group; †*P* < 0.05 versus DOCA-salt group.

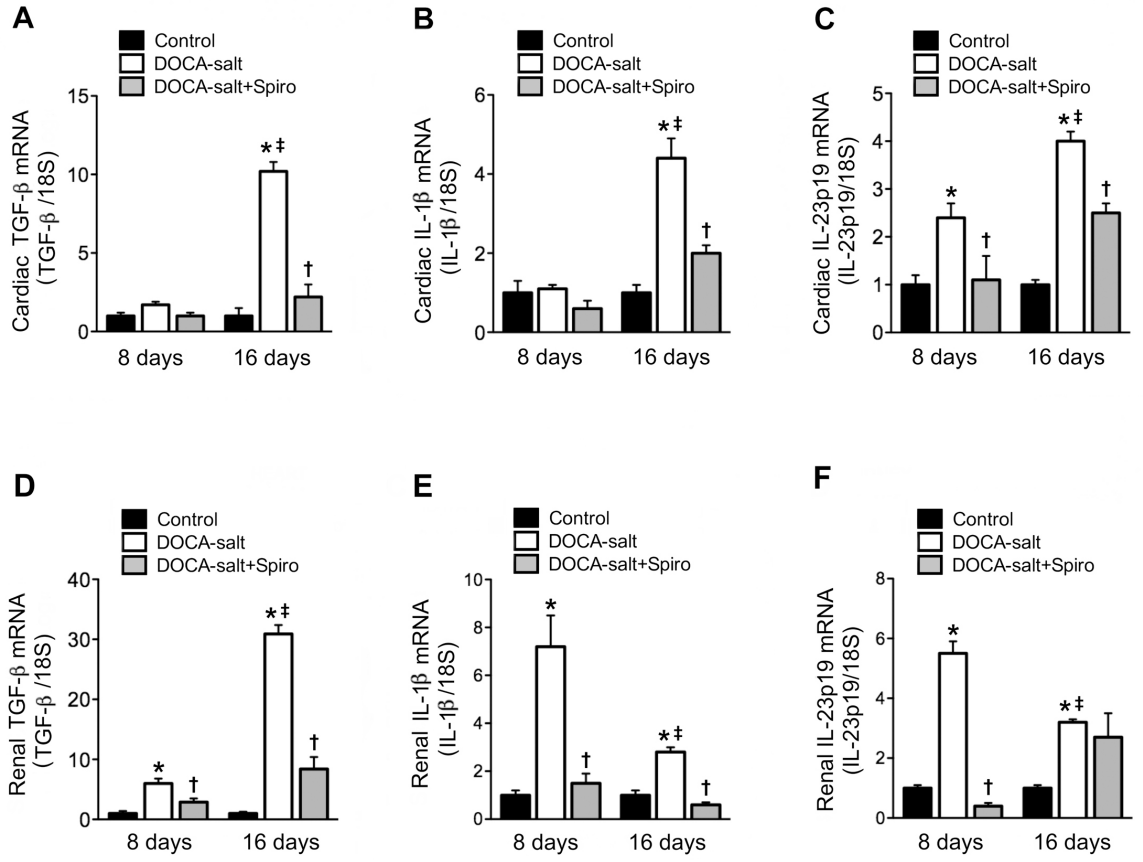

Figure S4. Effect of spironolactone on the expression of Th17 polarization/maintenance cytokines in heart and kidney of DOCA-salt rats. Transcript abundance estimated by qRT-PCR. (**A** and **D**) TGF-β1, (**B** and **E**) IL-1β, and (**C** and **F**) IL-23 (p19 subunit), in (**A**–**C**) heart and (**D**–**F**) kidney at 8 and 16 days of treatment. 18S rRNA was used to normalize abundance of mRNA. Data are expressed as average values ± SEM (n=5) *P < 0.05 versus value of control group; †P < 0.05 versus DOCA-salt group; ‡P < 0.05 versus DOCA-salt, at 8 days of treatment.

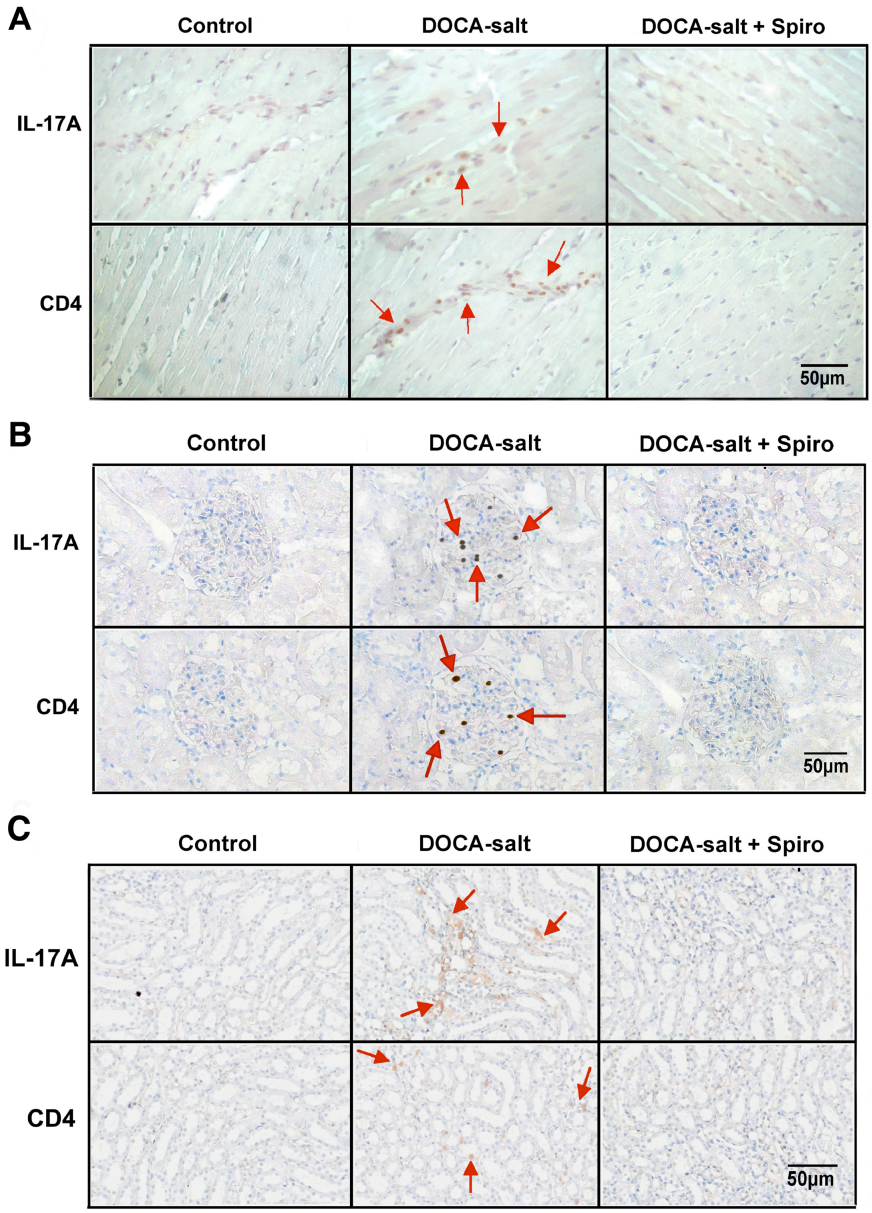

Figure S5. Infiltration of IL-17$^+$ and CD4$^+$ cells in heart and kidney of DOCA-salt rats. Immunohistochemistry of IL-17A (upper panels) and CD4 (lower panels) in (A) heart of DOCA-salt rats (after 16 days of treatment), and in kidney of DOCA-salt rats after 8 (B) and 16 days (C) of treatment. Arrows indicate positive signals for IL-17A and CD4. Scale bar=50 μm.

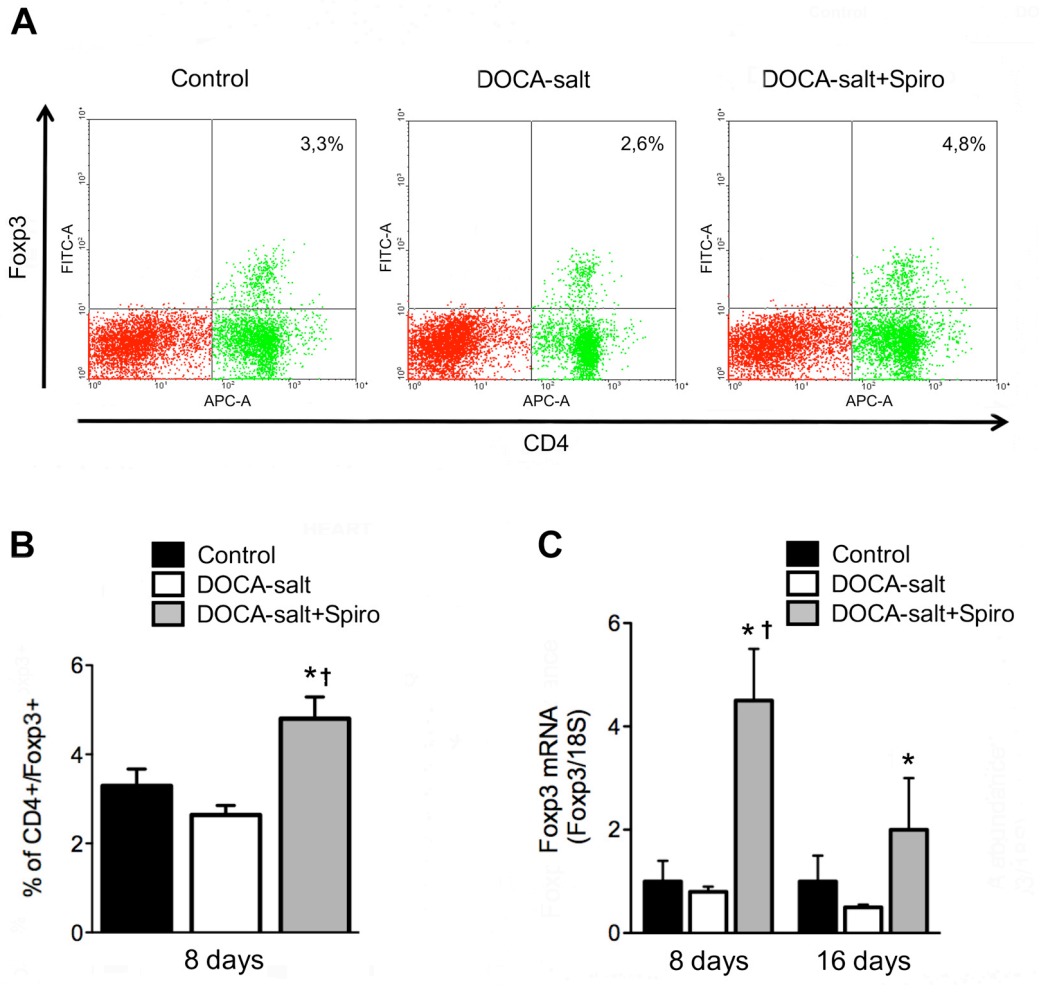

Figure S6. Spironolactone upregulates Foxp3 in spleen of DOCA-salt rats. (**A**) Flow cytometry of $CD4^+/Foxp3^+$ cell population in spleen and (**B**) quantification, at 8 days of treatment. Data are expressed as average values ± SEM (n=7). qRT-PCR for Foxp3 in (**C**) spleen, at 8 and 16 days of treatment. 18S rRNA was used to normalize abundance of Foxp3 mRNA. Data are expressed as average values ± SEM (n=5). **P* < 0.05 versus value of control group; †*P* < 0.05 versus DOCA-salt group.

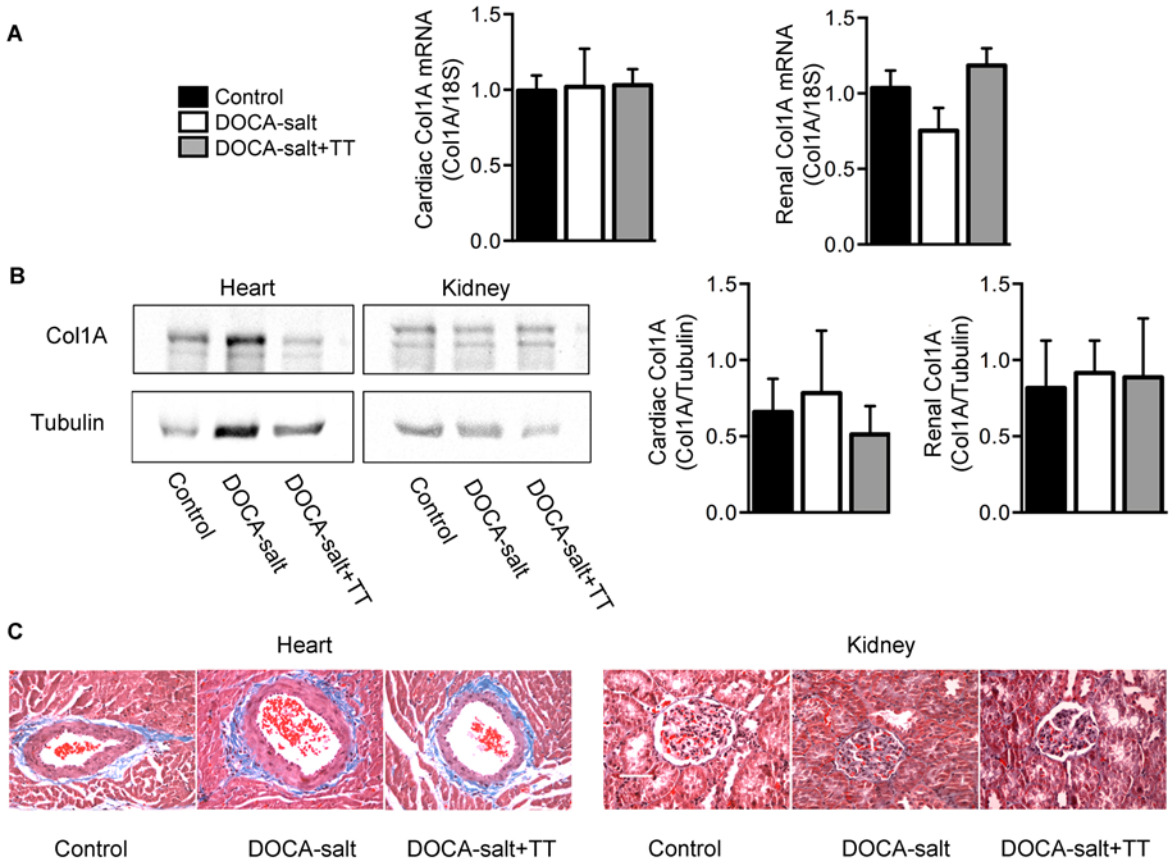

Figure S7. Effect of triple antihypertensive therapy (TT) in cardiac and renal fibrosis of DOCA-salt rats. (**A**) qRT-PCR for Col1A, in heart and kidney of control, DOCA-salt and DOCA-salt+TT rats. (**B**) Col1A protein abundance measured by Western blot and using tubulin as loading control in heart and kidney from control, DOCA-salt and DOCA-salt+TT rats. Bars represent mean±SEM (n=4). (**C**) Representative Masson's trichrome histological staining of heart and kidney from control, DOCA-salt and DOCA-salt+TT rats. Scale bar=30 μm.

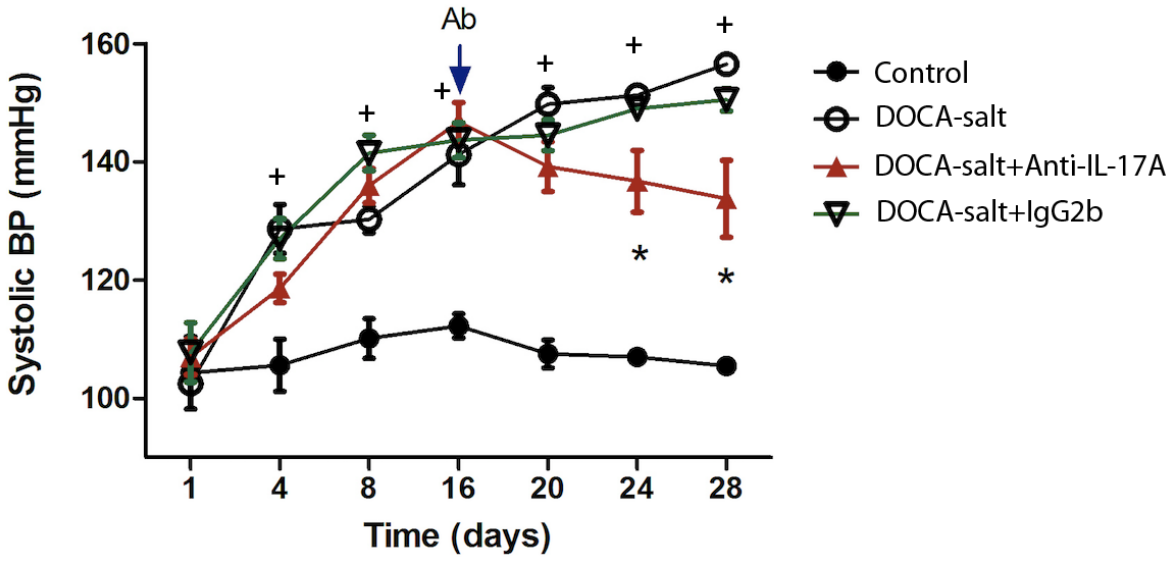

Figure S8. Effect of Anti-IL-17A treatment on systolic blood pressure in DOCA-salt rats. Arrow indicates the beginning of treatment of DOCA-salt rats (Protocol 3, new set of animals) with Anti-IL-17A or control IgG2b. Data are expressed as average values ± SEM (n=4 animals per group). +$P < 0.05$ vs Control; *$P < 0.05$ of DOCA-salt+Anti-IL-17A vs DOCA-salt+IgG2b.

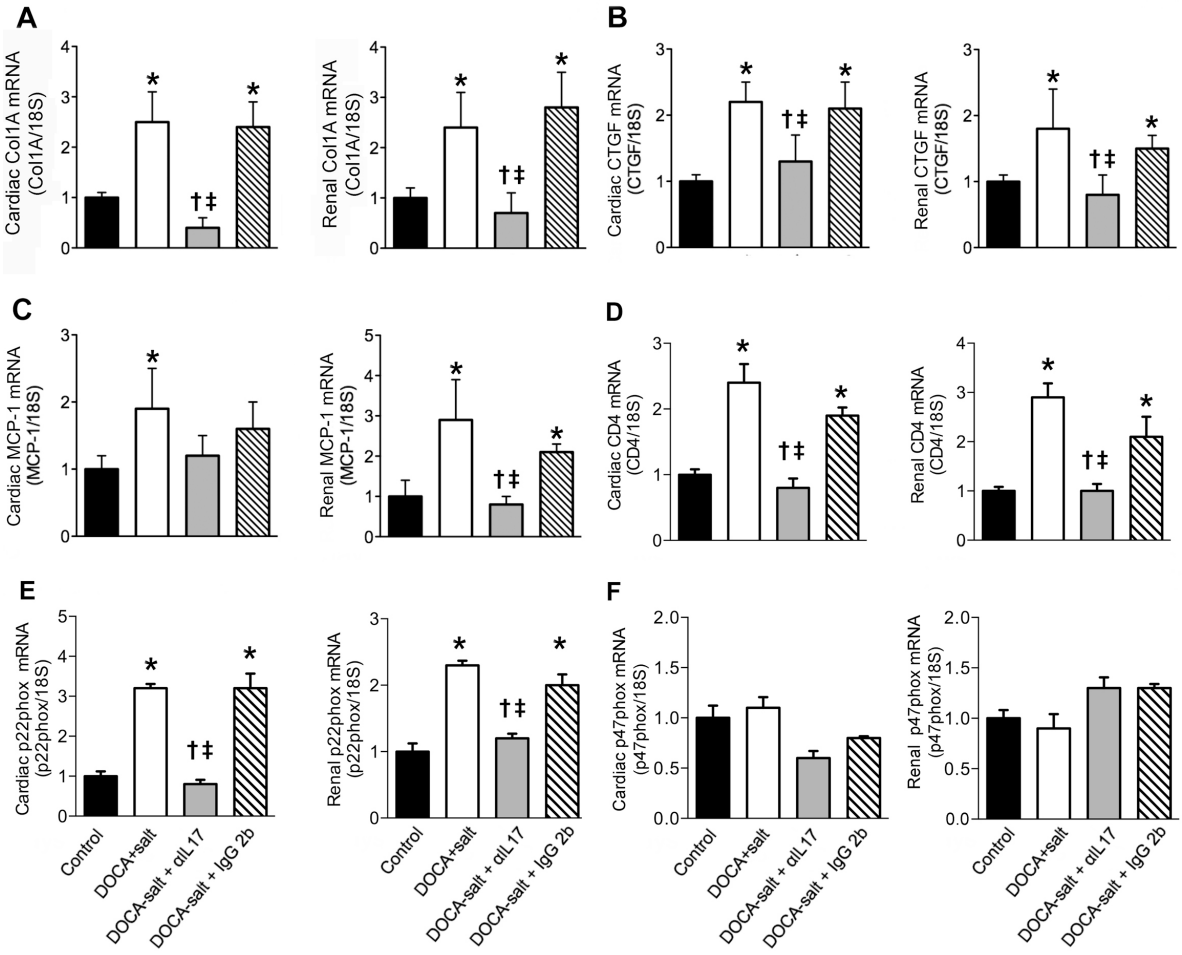

Figure S9. **Effect of systemic blockade of IL-17A in DOCA-salt rats.** qRT-PCR in heart and kidney for: (**A**) Col1A, (**B**) CTGF, (**C**) MCP-1, (**D**) CD4, (**E**) p22phox and (**F**) p47phox at 28 days of treatment. 18S rRNA was used to normalize abundance of mRNA. Data are expressed as average values ± SEM (n=8) **P* < 0.05 versus value of control group; †*P* < 0.05 versus DOCA-salt group; ‡*P* < 0.05 versus DOCA-salt+IgG2b group.

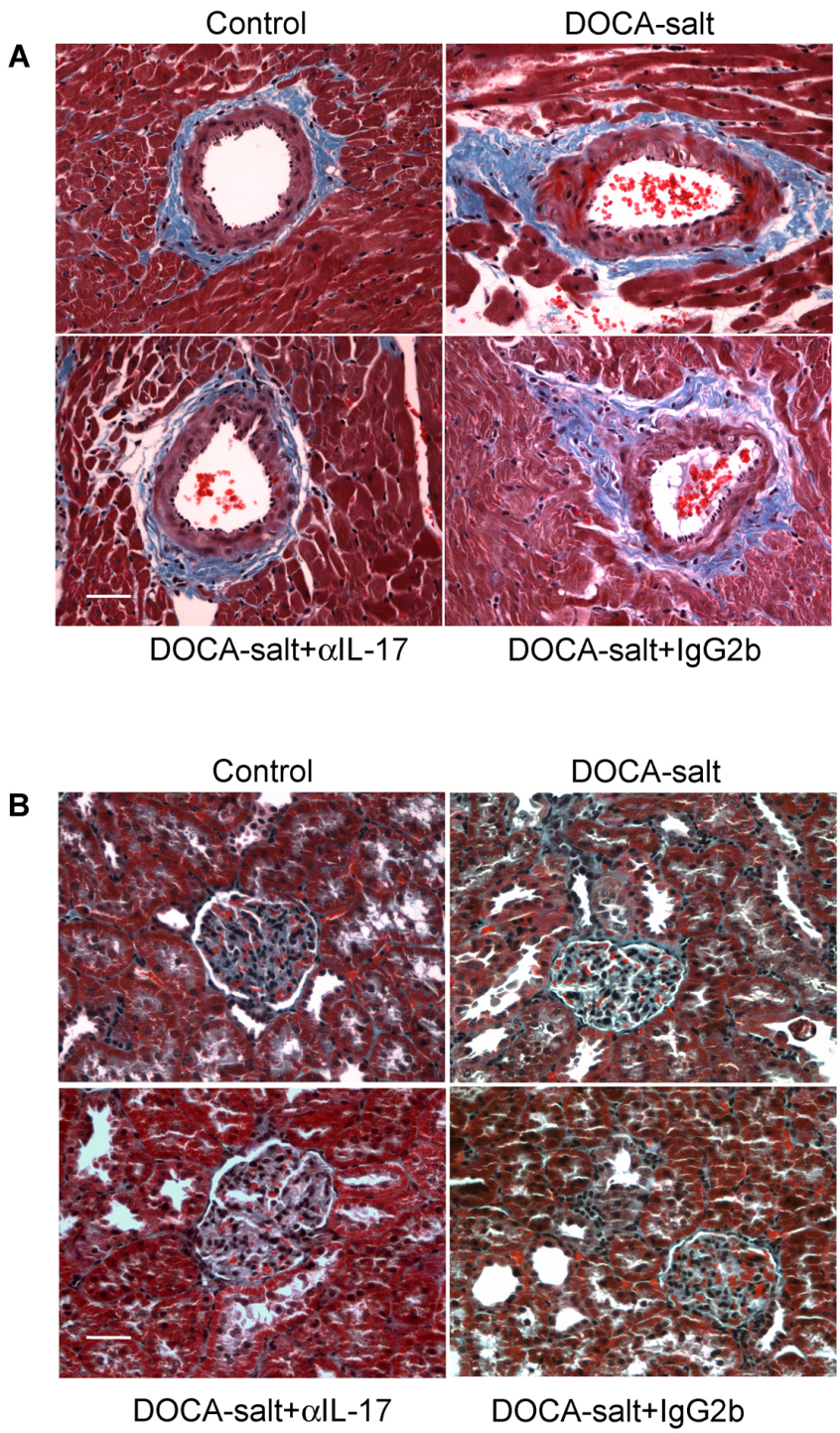

Figure S10. Effect of systemic blockade of IL-17A in cardiac and renal fibrosis of DOCA-salt rats. Representative Masson's trichrome histological staining of (**A**) heart and (**B**) kidney from control, DOCA-salt, DOCA-salt+Anti-IL-17 and DOCA-salt+IgG2b rats. Scale bar=30 μm.